

**The Electrical Properties of Natural Soil in the West Bank**  
**Dr. Mohammed M. Abu-Samreh \***  
**A. M. Saleh \***

---

**ABSTRACT**

In this study, the electrical properties of some soil samples in the West Bank have been investigated. Measurements were made from 100 Hz to 30 MHz between the temperatures of 293 K and 473 K and for fractional water contents of ~ 0 to 60%. The electrical conductivity is found to be highly dependent on the type of the soil, water contents and the exchangeable ions. Temperature also was found to play a significant role in the dielectric losses. The obtained data were found to fit the zero frequency conductivity and Cole-Cole type dielectric relaxations. The electrical conductivity and all relaxations follow an Arrhenius temperature dependence type whose activation energies increase with decreasing water content. Thus, increasing temperature at fixed water content will shift the electrical losses to higher frequencies.

**Keywords** Dielectric; Maxwell-Wagner; Soil; Clay; Arrhenius; frequency Dependence.

---

\* Al-Quds University, College of Science and Technology, Department of Physics, Abu-Deis, East Jerusalem, P O Box 20002, Palestine.

## **INTRODUCTION:**

Soils are not homogeneous media; rather they are composites of various constituents. As a major soil class is clays. Clays are composed of two-dimensional sheets of silicon-oxygen tetrahedral (silica sheets) and two-dimensional arrays of aluminum-or magnesium-oxygen-hydroxyl octahedral (alumina or magnesia sheets) (Van Olphen, 1963). The major types of clays are the two and three layered sheets. The montmorillonite clay type is an example of the three layer sheets, being composed of two silica sheets per each alumina sheet. The general formula for montmorillonites is (Mering, 1945):



where  $x+y \sim 0.33-0.5$  and M represents a monovalent ion such as Na. The substitution of lower valence ions for Al+3 in the alumina sheets and for Si+4 in the silica sheets results in an overall negative charge for these sheets which is neutralized by the coordination of cations (Smith and Hinchee, 1993). The ability of clay to take up mobile cations is characterized by the cation exchange capacity (CEC), which is defined as the number equivalent of exchangeable positive ions in units of mmole (or meq) per 100 g of soil (Iben, et al., 1996). A typical CEC for montmorillonite is between 60-100 meq/100g. The addition of water results in two effects. One is that the exchangeable ions can dissolve in the water. The other is that water can bind tightly to the surface of the silica layers, causing intra-crystalline swelling. The uptake of water and the thermodynamic release of the water depend strongly on the particular ion involved (Hendricks et al., 1940). In general, though, montmorillonite can take up an equal amount of water to clay, with an amount of tightly hydrated water being approximately 1g of H<sub>2</sub>O to 10g of clay. Differential thermal analysis of air dried montmorillonite powder with various cations coordinated to the clay show a single broad endothermic reaction centered at ~160 °C for the hydrogen, sodium, potassium, and cesium forms which is attributed to dissociation of hydrated waters (von Hippel, 1974; Calvet, 1975; Vinegar, et al., 1984; de Lima, et al., 1992). The lithium and calcium forms, though, showed a second, weaker endothermic reaction at ~240 °C which is attributed to the dissociation of waters coordinated to the divalent ions (Hendricks, et al., 1940)

Kaolinite clays are classified as two-layer clays formed of a one-to-one ratio of silica to alumina sheets (van Olphen, 1963). Kaolinites are much more homogeneous than montmorillonites, having many fewer isomorphous

substitutions and thus a lower CEC of ~1-10 meq/100g. For this reason, kaolinites are much less hydrophilic than are montmorillonites and do not form as strong an interaction with water. For the dried powder form of kaolinites, no endothermic reactions are observed until about 600 °C where irreversible dehydroxylation occurs.

Sand, which is composed primarily of silicon dioxide is a low loss material (Von Hippel, 1974; Corning, 1972). For dry soils, it is the minerals, clays and salts which contribute to the electrical losses. Two common minerals are the non-magnetic iron-III oxide hematite, Fe<sub>2</sub>O<sub>3</sub>, and the magnetic iron-II-III oxide magnetite, Fe<sub>3</sub>O<sub>4</sub>. Ca, Na and Fe salts are also prevalent in nature (Bresler, et al., 1982)

Investigations of soil electrical properties are of great importance in order to determine the viability and frequency range for direct heating with electromagnetic energy (e.g. 60 Hz, RF, or microwaves, MW). For instance, an understanding of the dielectric properties of soil is essential for determining which types of soils can be remediated using radio frequency (RF) heating. The remediation of soils contaminated by organic wastes either from spills or from old waste dumps is an important environmental issue. Various approaches have been utilized such as soil washing, the use of bio-organisms to decompose the wastes, steam vapor extraction, incineration, and thermal desorption (Smith and Hinchee, 1993)

In this study, the conductive and dielectric properties of various major classes of soils from the West Bank. The collected samples are classified into three major classes according to their components. The northern, middle and the southern soil samples are classified as sand, montmorillonite, and kaolinite clay, respectively (Von Hippel, 1974; Calvet, 1975; Vinegar, et al., 1984; de Lima, 1992). Thus, various major classes of soils have been targeted in this study, and the effect of temperature, water content and salt concentrations on the dielectric properties of montmorillonite and kaolinite clays have been investigated. Besides, the effect of temperature, salt, and water as well as the temperature dependence of the iron oxides hematite and magnetite in sandy soil and have developed a model to predict the real and the imaginary components of the permittivity.

### **Theoretical:**

The contributions to the dielectric properties of a soil can be obtained from various sources of soil. A mobile ion in an electrolyte or in the hydrated layers of a clay particle will contribute to the conductivity of the medium in which it resides. In general, a medium can be described by an effective total current conductivity,  $\sigma^*$ , given by a zero-frequency conductivity,  $\sigma$ , plus a

complex term, frequency-dependent dielectric susceptibility,  $\varepsilon(\omega)$ , the later of which has real and imaginary components (Kittel, 1996:(

$$\sigma^* = \sigma + j\omega\varepsilon(\omega) = \sigma + j\omega[\varepsilon'(\omega) - j\varepsilon''(\omega)] \quad (2)$$

( $\omega$  is the angular frequency in rad/sec and  $j=\sqrt{-1}$ ). A general expression for the dispersion of  $\varepsilon(\omega)$  of a medium can be characterized by a Cole-Cole type relaxation function (Smith and Hinchee, 1993; Cole and Cole, 1941):

$$\varepsilon(\omega) = \varepsilon_\infty + \frac{\Delta\varepsilon_q}{(1 + (j\omega\tau_q)^{\alpha_q})} \quad (3a)$$

$$\varepsilon(\omega)' = \varepsilon_\infty + \sum_q \Delta\varepsilon_q \left[ \frac{1 + \cos\left(\frac{\alpha_q\pi}{2}\right)(\omega\tau_q)^{\alpha_q}}{1 + (\omega\tau_q)^{2\alpha_q} + 2\cos\left(\frac{\alpha_q\pi}{2}\right)(\omega\tau_q)^{\alpha_q}} \right] \quad (3b)$$

$$\varepsilon(\omega)'' = \varepsilon_\infty + \sum_q \Delta\varepsilon_q \left[ \frac{\sin\left(\frac{\alpha_q\pi}{2}\right)(\omega\tau_q)^{\alpha_q}}{1 + (\omega\tau_q)^{2\alpha_q} + 2\cos\left(\frac{\alpha_q\pi}{2}\right)(\omega\tau_q)^{\alpha_q}} \right] \quad (3c)$$

$$\sum_q \Delta\varepsilon_q = (\varepsilon_L - \varepsilon_\infty) \quad (3d)$$

Where  $\varepsilon_\infty$  and  $\varepsilon_L$  are the high and low frequency values of the dielectric coefficient,  $\Delta\varepsilon_q$  is the contribution of the  $q^{\text{th}}$  relaxation to the dielectric dispersion  $\tau_q$  is the average dielectric relaxation time of the  $q^{\text{th}}$  relaxation phenomenon. The parameter  $\alpha_q$  represents a distribution of relaxation times. The general behavior of  $\alpha_q$  is as follows: for a distribution of relaxation times,  $\alpha_q < 1$ ; while for a single relaxation time (Debye relaxation),  $\alpha_q = 1$  (Smith and Hinchee, 1993). Since the contribution to the permittivity by a material is proportional to the amount of material  $\Delta\varepsilon_q$  and  $\varepsilon_\infty$ , from equation (3a),  $\Delta\varepsilon_q$  can be expressed as:

$$\Delta\varepsilon_q = \rho_q \delta\Delta\varepsilon_q \quad (4a)$$

$$\varepsilon_\infty = 1 + \sum_q \rho_q \delta\Delta\varepsilon_{\infty,q} \quad (4b)$$

Where  $\rho_q$ ,  $\rho_q \delta \epsilon_{\infty, q}$  and  $\rho_q \delta \Delta \epsilon_q$  are the relative density, the high frequency permittivity and the magnitude of the dielectric relaxation for the qth soil type .

Let us now introduce the impedance of coaxial cylinders. Such device is made of two copper tubes of length d and of a and b as an inner and outer radii, respectively. We shall treat the soil as having effective dielectric parameters. The electric current density, J, is proportional to the electric field,  $E = E_0 e^{j\omega t}$ , as follows (Kittle, 1996):

$$J(\omega, t) = \sigma^* E_0 e^{j\omega t} = [\sigma + j\omega \epsilon(\omega)] E_0 e^{j\omega t} \quad (5)$$

Where  $\sigma^*(\omega)$  is the total current conductivity,  $\sigma$  is the zero-frequency conductivity, t is time, and  $\epsilon(\omega) = \epsilon'(\omega) - j\epsilon''(\omega)$  is the effective complex dielectric constant. For a coaxial cylinder with the annulus filled with a lossy dielectric medium, the wave Equation for the magnetic, H, and electric, E, fields excited at the radial frequency  $\omega$  reduces to the following (Lorrain and Corson, 1970; Gray, 1957):

$$(k^2 + \omega^2 \epsilon \mu \epsilon_0 \mu_0 \sigma) \left[ \frac{\vec{H}}{\vec{E}} \right] e^{j(\alpha \pm kz)} = 0 \quad (6)$$

Where z is distance along the coaxial axis.  $\sigma$  is conductivity and  $\epsilon$ , and  $\mu$  are respectively the dielectric constant and the magnetic permeability. The complex wave vector, k ( $= 2\pi/\lambda$ , with  $\lambda$  being the complex wavelength within the medium), and its real and imaginary parts are determined by the solution to equation (6), as given by equations (7a-d).

$$k = \sqrt{\frac{\omega^2 \epsilon \mu}{c^2} - j\omega \mu \mu_0 \sigma} = k' - jk'' \quad (7a)$$

$$k' = \left[ \frac{\omega}{c} \sqrt{\mu' \epsilon'} \right] \sqrt{\frac{\sqrt{(1 + \delta^2)} + 1}{2}} \quad (7b)$$

$$k'' = \left[ \frac{\omega}{c} \sqrt{\mu' \epsilon'} \right] \sqrt{\frac{\sqrt{(1 + \delta^2)} - 1}{2}} \quad (7c)$$

$$\delta = \frac{(\sigma + \omega \epsilon'' \epsilon_0)}{\omega \epsilon' \epsilon_0} \quad (7d)$$

In the above equations, the dielectric constant has been separated into its real and imaginary components:  $\epsilon(\omega) = \epsilon'(\omega) - j\epsilon''(\omega)$  . Other than magnetite,  $\mu$  is set equal to its vacuum value, and for magnetite,  $\mu = 1.06 \mu_0$  (von Hippel, 1954). In equation (7d),  $\delta$  represents the loss tangent and is defined as the ratio of dissipative to stored energy in a traveling wave.

For an open ended coaxial cylinder with the inner and outer radii of  $a$  and  $b$ , respectively, and a length  $d$  filled with a lossy medium, the impedance,  $Z$ , can be written as (Gray, 1957):

$$Z = Z' + jZ'' = k \left( \frac{\ln\left(\frac{b}{a}\right)}{2\pi} \right) \left( \frac{\cot(kd)}{\sigma + j\omega\epsilon\epsilon_0} \right) + j\omega L_{lead} \quad (8)$$

$Z'$  and  $Z''$  the real and imaginary components of the impedance  $L_{lead}$  (~15 nh) is the inductance of the leads connecting wire to the coaxial line. The lead inductance adds up to the measured impedance a complex term of  $Z_{lead} = j\omega L_{lead}$  which was also used in the calculation of the total impedance. For the low loss, long wavelength cases, an effective permittivity for the sample,  $\epsilon'$  and  $\epsilon''$ , and the loss tangent can be easily expressed from the raw data of  $Z'$  and  $Z''$

$$\epsilon' = - \left( \frac{\ln\left(\frac{b}{a}\right)}{2\pi d \omega \epsilon_0} \right) \left( \frac{Z'' - \omega L_{lead}}{Z'^2 + (Z'' - \omega L_{lead})^2} \right) \quad (9a)$$

$$\epsilon'' = \left( \frac{\ln\left(\frac{b}{a}\right)}{2\pi d \omega \epsilon_0} \right) \left( \frac{Z'}{Z'^2 + (Z'' - \omega L_{lead})^2} \right) - \frac{\sigma}{\omega \epsilon_0} \quad (9b)$$

$$\delta = \frac{Z'}{Z'' - \omega L_{lead}} \quad (9c)$$

## EXPERIMENTAL:

Soil samples were collected from various places in the West Bank. The test site samples were 1.14-1.82 g cm<sup>-3</sup> of dry soil from different zones. The montmorillonite, and kaolinite samples were obtained from natural clays. The clays are then slurred in a dilute acid followed by a water slurry and drying. The result of the acid slurry was to replace the exchangeable ions with H<sup>+</sup> ions. The acid also chewed up a substantial fraction of the exchangeable sites so that the CEC for the montmorillonite clay was about 30 meq/100g as compared to its normal range of 60-100 meq/100g. Table 1 gives the CEC of the samples as measured by ammonium acetate and sodium acetate exchange, NaOH exchange (for the H<sup>+</sup> contribution) and by conductometric titration with Ba<sup>+2</sup> (Mehlich, 1948). The thermodynamic

properties, as measured by differential scanning calorimetry, of the montmorillonite and kaolinite clays (Hendricks, et al., 1940). The clay samples were mixed with distilled water and an amount of salt was added to the soils. The M-montmorillonites, where M represents a metal, were formed made by titrating the H-montmorillonite with MOH until the pH was 8.1 (Hendricks, et al., 1940). The dielectric properties of the soils studied were investigated by measuring the impedance of a coaxial line whose annulus was filled with the soil under investigation. The coaxial line was made of two copper tubes 30 cm in length. The inner tube had an outer diameter of 3.4 cm and the outer tube had an inner diameter of 6.6 cm. A brass flange was silver soldered to the base of the outer conductor to which a solid quartz disk was bolted. The quartz disk served holds the soil inside the annulus and to center the tubes. Quartz was chosen due to its low dielectric loss (loss tangent  $< 2 \times 10^{-4}$  up to 120 °C) (Corning, 1972). The phase and the magnitude of the impedance of the coaxial line were measured using a Hewlett Packard model HP4194 impedance analyzer.

The temperature was maintained using 60 Hz electric heating tape and controlled by a temperature controller. The temperatures outside and inside the coaxial line were monitored using type K thermocouples. A fiberglass blanket was wrapped around the coaxial line for thermal insulation. The weight of the samples was measured using a balance (Mettler model PM16-M, accuracy 0.1 g).

## **RESULTS:**

For an empty coaxial test, transforming of the impedance and phase into  $\epsilon'$  and  $\delta$  will be resulted in  $\epsilon'$  of 1.11 between 100 Hz and 10 MHz, which rose to 1.19 by 30 MHz due to lead induction.  $\epsilon''$  is about 0.5 at 100 Hz and falls inversely with frequency to the 0.67 power to about  $10^{-3}$  at 100 kHz. From 100 kHz to 30 MHz,  $\epsilon''$  is below  $10^{-3}$ . Thus for a low loss sample, the resolution in  $\delta$  is  $10^{-3}$  for frequencies above 100 kHz.

### **Results of Sand with electrolyte:**

The total current conductivity of sand with an electrolyte is dominated by the conductivity of salt until the concentration of the electrolyte falls below a value sufficient to sustain a continuous conduction path. Figure 1 shows the conductivity of sand with a Na-electrolyte at 100 °C as a function of water content. The dry sand density is  $1.35 \text{ g cm}^{-3}$  and has a porosity of

0.35. The Na content is  $0.19 \times 10^{-4}$  mole  $\text{cm}^{-3}$ . The water content,  $f_w$ , is given in water weight to dry soil weight, g:g. When fully saturated with water,  $f_w = 0.26$  g:g. The conductivity is found to fit an Arrhenius expression of the form:

$$\sigma = \exp \left[ A_\sigma - \frac{h_\sigma}{T} - \frac{1}{\beta_\sigma f_w + \Gamma_\sigma} \right] \quad (10)$$

The parameters used to obtain the best fit are:  $A_\sigma = 4.4$ ,  $h_\sigma = 1410 \pm 600$  °K,  $\beta_\sigma = 20.1 \pm 2.$ , and  $\Gamma_\sigma = 0.065 \pm 0.015$  (Iben, et al., 1996). For high water content,  $\sigma$  reduces to a constant value of 0.55 at 20 °C. This is 0.32 times the conductivity at 20 °C for a pure electrolytic solution of 0.19 mole/l of NaCl (Weast, 1975). The Arrhenius temperature dependence of the conductivity is indicative of a process with activation energy such as ionic diffusion.

Figures 2a-b show the dispersion curves for water contents of  $f_w \sim 0.8$  mg:g (1.4, 0.5, 0.3 g H<sub>2</sub>O and sand is 906 g) at 75 °C, 140 °C and 145 °C. The data were fit with the following dispersion equations:

$$\tau_1 = \frac{\Delta \varepsilon_1 \varepsilon_0}{\delta_1 \sigma} \quad (11a)$$

$$\Delta \varepsilon_1 = \frac{\delta_1 \sigma \tau_1}{\varepsilon_0} \quad (11b)$$

The dispersion in equation (11b) depends only one single relaxation time, ( $\tau_1$ ), and it has a magnitude of  $13.5 \pm 2.1 \varepsilon_0$ , that can be obtained using the following parameter values:  $\alpha_1 = 0.5$ ,  $\delta \varepsilon_{\infty,1} = 1.15 \varepsilon_0$  per  $\text{g cm}^{-3}$ , and  $\varepsilon_0 = 2.55 \varepsilon_0$ . The product of  $\langle \sigma \tau_1 \rangle \sim 31.8 \varepsilon_0$ , so that the magnitude  $\Delta \varepsilon_1 \sim 0.42 \langle \sigma \tau_1 \rangle$ , and  $\tau_1 \sim (1/\sigma) \times 2.7 \pm 1.5 \times 10^{-10}$  sec  $\Omega^{-1}$  m. Once the water has been completely evaporated, the effective conductivity drops to the order of  $10^{-9}$  mhos  $\text{m}^{-1}$ , and  $\tau_1$  becomes long. The low amount of water ( $1.1 \text{ mg cm}^{-3}$ ) is clearly not enough to be responsible for the effective dielectric loss observed. Since water has a dielectric coefficient of  $79 \varepsilon_0$  per  $\text{g cm}^{-3}$ ,  $1.1 \text{ mg cm}^{-3}$  would result in a dielectric value of  $0.09 \varepsilon_0$ , or 150 times weaker than the magnitude observed. Rather, the effective dielectric loss is due to a Maxwell-Wagner relaxation due to needles of conducting water pockets in the insulating sand medium and it is generally expressed in its general as in equation (11a) (Sillars, 1937).

### **Results of clays:**



Relatively speaking, the dielectric losses of clays are all complex according to the number of observable relaxation processes and in their dependence on  $f_w$ . The number and type of observed dielectric relaxations of kaolinite and montmorillonite clay are the same, but their magnitudes and the dependence on temperature and water contents are completely different. Three different regimes can be identified for the dispersion of clays on the basis of water contents: (I) high, (II) intermediate, and (III) low water contents. We shall discuss the results belong to each region separately. Furthermore, the transition between the high and low water content is not abrupt but is continuous. The water contents distinguishing the three regimes are dependent on the type of clay and the exchangeable salt.

In high water content, additional waters or unbound water is expected to be presented. Wet soil contains free waters in which the exchangeable cations can flow. For montmorillonite clay, regime I is for  $f_w > 0.15$  g:g and for kaolinite clay, regime I is for  $f_w > 0.3$  g:g. The conductivity versus fractional water content is shown in Figure 1 for montmorillonite clay with Na, Ca and H as the exchangeable ion and for H-kaolinite clay. The results have shown that, the conductive and dielectric properties of the clays are dominated by ionic conductivity for high concentrations of water. The observed two Maxwell-Wagner relaxations which were attributed to the differences in conductivity of the clay particles and the electrolytic water solution which results in a buildup of ions at interfacial barriers (Calvet, 1975; de Lima, et al., 1992). The dependence of the conductivity of a single ion species on temperature and on water content can be expressed as follows:

$$\sigma(f_w) = \exp \left[ A_\sigma - \frac{h_\sigma}{T} - \beta_\sigma(f_w) f_w \right] \quad (12)$$

Where  $h_\sigma$  is the enthalpy expressed in degrees Kelvin ( $h_\sigma = H_\sigma / k_B$  where  $H_\sigma$  is the enthalpy in energy units and  $k_B$  is the Boltzmann constant),  $f_w$  is the ratio of the water content to the clay content,  $\exp(A_\sigma)$  is the extrapolation of the conductivity to zero water content and infinite temperature within the given range of water contents,  $\beta_\sigma(f_w)$  will be linear, but with decreasing water content,  $\beta_\sigma(f_w)$  will increase dramatically. The strong dependence of the bulk conductivity on water content is due to the disruption of a continuous path for ion flow and it follows an Arrhenius behavior.

Figure 3 a shows the real part of the permittivity for Na-montmorillonite with a density of  $0.29 \text{ g cm}^{-3}$  versus fractional,  $f_w$ , water content between 0.65 g:g and 0.10 g:g. Clearly, two relaxation processes are observed.

These processes are introduced as  $\alpha_0$  and  $\alpha_1$ . The obtained data are in good agreement with the Cole-Cole relaxation functions and the frequency independent conductivity. The data for  $f_w = 0.65$  is fit using equations (3a-d) with two relaxation functions,  $\alpha_0$  and  $\alpha_1$ . The  $\alpha_0$  relaxation is associated with diffusion of ions (Na in this case) across the clay particles and building up at the clay-electrolyte boundary, which is termed membrane-bound polarization. This leads to a large capacitive effect due to the thinness of the interfacial barrier (1-100 nm), resulting in a value of  $\Delta\epsilon_0$  of the order of  $10^5$ . For membrane bound polarizations, the magnitude of the relaxation,  $\Delta\epsilon_0$ , is proportional to the product of the conductivity times the relaxation time with a proportionality coefficient of  $\delta_1=0.13$ , (Equation (11b)). The second, weaker relaxation process, termed the  $\alpha_1$  process, is also a Maxwell- Wagner relaxation due to the interfacial polarization at the clay-electrolyte interface, but the frequency is too high for the ions to diffuse across the dimensions of the clay. The relaxation time for a Maxwell-Wagner relaxation is given by equation (11a) using equation (12) for the conductivity, and assuming  $\Delta\epsilon_q = \text{constant}$ . The much shorter relaxation times for  $\alpha_1$ ,  $\tau_1$ , compared to  $\alpha_0$  are a result of the much lower effective dielectric coefficient of the clay particles and their environment at frequencies  $f \gg 1/2 \pi\tau_0$  (Note that for water,  $\epsilon' = 79$  up to  $\sim 1\text{GHz}$ ).

The intermediate regime bridges the high and low regimes and is not a distinct regime, but is used only for simplicity of describing the transition. This type of region is defined as the range of  $f_w$  where  $\beta_{\sigma f_w}$  becomes dramatically more negative with decreasing  $f_w$  due to a disruption of the continuous conductive path. For montmorillonite clays,  $f_w \sim 0.1 \text{ g:g}$  to  $0.15 \text{ g:g}$  and for kaolinite clay, this is for  $f_w \sim 0.3 \text{ g:g}$ . In the case of montmorillonite clays, the free water has been removed and the clay can now be heated to above the  $100^\circ\text{C}$  to  $110^\circ\text{C}$  threshold for bulk water evaporation. For kaolinite clay and sand, free water still remains to be boiled off. In this regime,  $\sigma$  is so low that the membrane-bound polarization relaxation,  $\alpha_0$ , is essentially gone, having been shifted to very low frequencies (equations (11 a-b)). Thus  $\Delta\epsilon_0$  and  $\tau_0$  are ill defined since  $(2\pi 100 \text{ Hz}) \tau_0 \gg 1$  and the fits, though, only determine the following relationship between the parameters:

$$\left[ \frac{\Delta\epsilon_q}{(\omega_{\min} \tau_q)^{\alpha_q}} \right] = \text{constant} \quad (13)$$

Where  $\omega_{\min} = 2\pi \times 100$  Hz in our experiments and  $q=0$  for the  $\alpha_0$  relaxation. For continuity, the magnitude of  $\Delta\epsilon_0$  is maintained at its value in region I.

Figures 4a-b show the temperature dependence of  $\epsilon'$  and  $\delta$  for H-montmorillonite clay with a density of  $0.43 \text{ g cm}^{-3}$  for a temperature range between  $25 \text{ }^\circ\text{C}$  and  $150 \text{ }^\circ\text{C}$  with  $f_w = 0.026 \text{ g:g}$ . A new relaxation,  $\alpha_2$ , now appears. (H-montmorillonite is shown since  $\alpha_2$  is a distinct relaxation where as for Na-montmorillonite, the  $\alpha_1$  and  $\alpha_2$  relaxations are smeared together as one relaxation).  $\alpha_1$  is the same Maxwell-Wagner relaxation observed in the high water content regime. The conductivity, though, has dropped so that  $\tau_0$  has essentially disappeared and  $\tau_0$  has shifted to low frequencies. The data can be fit using equations (3a-d) or (4a-b) with  $q = 1$  and  $2$ , and with temperature dependent relaxation times,  $\tau_1$  and  $\tau_2$ . The dependence of the relaxation time,  $\tau_q(T, f_w)$ , on temperature and water content can also be expressed as:

$$\tau_q(T, f_w) = \exp\left[\frac{A_q(f_w) + h_q(f_w)}{T} - \beta_q(f_w)f_w\right] \quad (14)$$

The dependence of the relaxation times on temperature is shown in Figure 4c. Ca-montmorillonite shows a very similar dispersion curve to that of H-montmorillonite.

In the low water content regime, all waters present are bound to the clay surfaces (hydration) and the effect of different ions is dramatic. Hydrated montmorillonite clays have a thermodynamic transition at around  $160 \text{ }^\circ\text{C}$  which involves the dehydration of interstitial waters. At temperatures of  $160 \text{ }^\circ\text{C}$  and above, the hydrated water is evaporated. For both the H and the Ca forms of montmorillonite clay, the intensity of  $\alpha_2$  decreases with decreasing water content. This is seen for H-montmorillonite in Figures 5 a. The dispersion curve for Ca-montmorillonite is similar. The data can be fit by making  $\Delta\epsilon_2$  decrease with decreasing water content while  $\Delta\epsilon_1$  remains constant. Both  $\tau_1$  and  $\tau_2$  depend on temperature and water content as given by equations (14), but they are independent. Plots of  $\tau_1$  and  $\tau_2$  versus  $f_w$  are shown in Figures 5 b-c, respectively. A plot of  $\Delta\epsilon_2$  versus  $f_w$  is also shown in Figure 5c.  $\Delta\epsilon_2$  can be parameterized according to the expression:

$$\Delta\epsilon_2(f_w) = \Delta\epsilon_{2\infty} \exp[-\kappa_1 \exp(-\kappa_2 f_w)] \quad (15)$$

The parameters used to fit the dispersion curves for H-montmorillonite and Ca-montmorillonite are given in Table 4.  $\Delta\epsilon_{2\infty}$  is the high water content

value of  $\Delta\epsilon_2$ . With the complete loss of water, the losses for Ca and H-montmorillonite are similar in frequency dependence to those of sand, but are about a factor of 4 times higher in magnitude for the same density.

Let us discuss the effects of iron-oxides. In soils, the iron content is generally on the order of a few percent by weight and is usually present as an oxide. It was found that the frequency dependence of the dielectric relaxation for hematite is very broad. Figure 8 is an Arrhenius plot of  $\tau$  for hematite and shows that on heating the soil from 20 °C to 160 °C increases  $\tau$  by a factor of  $2.4 \times 10^3$ . Since hematite,  $\text{Fe}_2\text{O}_3$ , is a stable iron oxide with increased temperature, the losses in the MHz range will increase with increased temperature.

Another naturally occurring iron oxide is magnetite, which is magnetic and has very large dielectric losses. Figure 7 is a plot of  $\epsilon'$  at 150 °C include 1% (g:g) of magnetite in sand with a total density of  $1.35 \text{ g cm}^{-3}$ . For the low concentration limit, the magnitude of the dielectric relaxation is directly proportional to the mass density of magnetite particles as given by equation (4b-c). The data is fit using a single relaxation process for magnetite and two relaxations for sand and an Arrhenius temperature dependence for  $\tau$  (equation (14) with  $\beta(f_w) = 0$ ). We attribute the dielectric relaxation for magnetite either to a dipolar relaxation or a membrane-bound polarization. The Arrhenius temperature dependence of magnetite is shown in Figure 6 and shows that the peak frequency increases from Hz at 20 °C to 2 MHz at 160 °C.

## **DISCUSSION:**

The dielectric losses of soils are complex functions of clay, water, salt and mineral content as well as temperature. Dielectric losses of the predominant constituents of soil (sand and clays) are low in their pure dehydrated forms, the additions of even minor amounts of sodium salt and minerals greatly improves their in-phase coupling to radio frequencies (losses), in general. The  $\alpha_0$  and  $\alpha_1$  relaxations are present for all exchangeable ions, both for montmorillonite as well as kaolinite clay. Another important point is that the conductivity exhibits an Arrhenius temperature dependence indicating an activated process. Thus, increasing the temperature resulted in increasing  $\sigma$  and thus decreasing  $\tau_0$  and  $\tau_1$ .

In this study, it appears that, for clays, the dominant loss mechanism is due to ion mobility rather than a dipolar relaxation of polar molecules such as water. The losses are shifted to high frequencies via an interfacial polarization or Maxwell-Wagner mechanism, without which the losses at RF frequencies would be negligible. The composition of the clays with the bound negative charges and positively charged counter ions is essential for the membrane bound polarization effect, the  $\alpha_0$  relaxation, since an electrolytic solution mixed with sand does not display a membrane bound polarization effect. While the Maxwell-Wagner relaxation,  $\alpha_1$ , is observed for all hydrated soils possessing either clay or an electrolyte. The dependence of  $\tau_1$  on  $T$  and  $f_w$  is strongly dependent on the clay type and the specific counter ion. Furthermore, the magnitude and the extent of the frequency range of the losses both increase with increased CEC of the clay. From the dependence of the relaxation times versus water content, it is evident that even modest amounts of water increase the losses dramatically.

#### **REFERENCES:**

1. Arps, J. J., (1953). The effect of temperature on the density and electrical resistivity of sodium chloride solutions: *Petr. Trans. Am. Inst. Min., Metall. & Pet. Eng.*, 198, 327-330.
2. Corning Inc., October (1972). *Properties of Glasses and Glass-Ceramics*, Published in USA .
3. Bidadi, H., Schroeder, P. A. and Pinnavaia, T. J., (1988). Dielectric properties of montmorillonite clay films: effects of water and layer charge reduction: *J. Phys. Chem. Solids*, 49, 1435-1440.
4. Bolt, G. H. and Bruggenwert, M. G. M., Editors, (1978). *Soil Chemistry A. Basic Elements*. Elsevier Scientific Publishing Co., New York.
5. Bresler, E., McNeal, B. L., and Carter, D. L., (1982). *Saline and Sodic Soils*. Springer-Verlag, New York.
6. Calvet, R., (1975). Dielectric properties of montmorillonites saturated by bivalent cations: *Clays and Clay Minerals*, 23, 257-265.
7. Cole, K. S. and Cole, R. H., (1941). Dispersion and absorption in dielectrics. I. Alternating current characteristics: *J. Chem. Phys.*, 9,341-351.
8. de Lima, O. A. L. and Sharma, M. M., (1992). A generalized Maxwell-Wagner theory for membrane polarization in shaly sands: *Geophysics*, 57, 431-440.
9. Gray, D. E., coordinating editor, (1957). *American Institute of Physics Handbook*, McGraw- Hill Book Co., INC, New York, 5-36 to 5-51.

10. Helmy, A. K., Santamaria, R. M. and Garcia, N. J., (1989) Dielectric behavior of montmorillonite discs: *Colloids and Surfaces*, 34, 13-21.
11. Hendricks, S. B., Nelson, R. A. and Alexander, L. T., (1940). Hydration mechanism of the clay mineral montmorillonite saturated with various cations: *J. Am Chem. Soc.*, 62, 1464-1457
12. .1464-1457
13. Iben, I.E.T., Edelstein, W.A., and Roemer., P.B., (1996). Dielectric Properties of Soil: Application to Radio Frequency Ground Heating, Technical Information Series, Electronic Systems Laboratory Report Number 96CRD150 .
14. Kerr, P. F. and Kulp, J. L., (1948). Multiple differential thermal analysis: *The American Mineralogist*, 33, 387-419.
15. Kittel, C., (1996). *Introduction to Solid State Physics*, 7th edition, John Wiley & Sons, INC. New York.
16. Lorrain, P. and Corson, D. R., (1970). *Electromagnetic Fields and Waves*, 2nd edition, W. H. Freeman and Company, San Francisco.
17. Mehlich, A., (1948). Determination of cation-and anion-exchange properties of soils: *Soil. Sci.*, 66, 429-445.
18. Mering, J., (1945). On the hydration of montmorillonite: *Trans. Faraday Soc*, 42B, 205-219 .
19. Sillars, R. W., (1937), The properties of a dielectric containing semiconducting particles of various shapes: *Journal IEEE*, 80, 378-394.
20. Smith, L. A. and Hinchee, (1993). *In Situ Thermal Technologies for Site Remediation*, Lewis Publishers Boca Raton, Ann Arbor, London, Tokyo.
21. Smyth, C. P., (1955). *Dielectric behavior and structure*”, McGraw-Hill Book Company, Inc. New York, Toronto, London.
22. Vinegar, H. J. and Waxman, M. H., (1984). Induced polarization of shaly sands: *Geophysics*, 49, 1267-1287.
23. Van Olphen, H., (1963). *Clay Colloid Chemistry*, chapter 6: “Clay Mineralogy” 59-88.
24. von Hippel, A. R., ed., (1954). “Dielectric Materials and Applications, Papers by Twenty-two Contributors.” The Technology Press of M. I. T. and John Wiley & Sons, Inc., New York, Chapman & Hall, LTD., London.
25. Weast, R. C., editor, (1975-1976). *Handbook of Chemistry and Physics*, 56th edition. By CRC press, INC., Cleveland, Ohio.

**List of Tables:**

**Table 1. The CEC and the composition of exchangeable ions for the various samples.**

| sample/CEC | Ca | Mg | K | Na | Fe | H | sum | NH <sub>4</sub> OAc | Ba |
|------------|----|----|---|----|----|---|-----|---------------------|----|
|------------|----|----|---|----|----|---|-----|---------------------|----|

|                 |      |      |      |      |   |      |      |      |     |
|-----------------|------|------|------|------|---|------|------|------|-----|
| montmorillonite | 7.73 | 4.57 | 0.23 | 0.59 | 0 | 20.1 | 33.7 | 31.7 | 34  |
| kaolinite       | 0.92 | 0.15 | 0.01 | 0.79 | 0 | 2.6  | 4.46 | 5.9  | 6   |
| test site       | 9.6  | 0.44 | 0.06 | 0    | 4 | 0    | 10.1 | 4.1  | 4.4 |

**Figure Captions:**

- Figure 1 A plot of  $\sigma$  versus  $f_w$  for the  $Na^+$ ,  $H^+$ , and  $Ca^{2+}$  forms of montmorillonite clay with densities of 0.511, 0.384, 0.370  $gcm^{-3}$ , the  $H^+$  form of Kaolinite clay with a density of 0.665  $gcm^{-3}$ , and  $Na^+$ - sand (13.5 meq Na:100 g sand) with a density of 1.35  $gcm^{-3}$ .
- Figure 2 Plots of (a)  $\epsilon'$  and (b)  $\epsilon''$  versus frequency for 1.35  $g cm^{-3}$  sand with 13.5 meq Na:100g sand at  $f_w$  and T values of: 16  $\times 10^{-4}$  g:g and 75 °C;  $5.6 \times 10^{-4}$  g:g and 140 °C; and  $3.3 \times 10^{-4}$  g:g and 144°C.
- Figure 3 (a) Dispersion curve of  $\epsilon'$  for Na- montmorillonite with a density of 0.384  $g cm^{-3}$  at 100 °C for  $f_w = 0.65, .56, .49, .42, .34, .26, .21, .15$  and 0.09. The data for  $f_w = 0.65$  is fit using Equations 3a-d with two relaxation functions, alpha0 and alpha1.
- Figure 4. The temperature dependence of (a)  $\epsilon'$  and (b)  $\delta$  versus “scaled” frequency for H montmorillonite with a density of 0.511  $g cm^{-3}$  for the temperatures of 29 °C, 50 °C, 73 °C, 100 °C, 123 °C, and 150 °C with  $f_w = 0.029$  g:g. (c) An Arrhenius plot of  $\tau_1$  and  $\tau_2$  for 0511  $g cm^{-3}$  of H-montmorillonite.
- Figure 5 (a)  $\epsilon'$  versus frequency for 0.511  $g cm^{-3}$  of H-montmorillonite at 160 °C in region III for  $f_w = 21.2, 15.6, 13.2, 10.9, 9.7, 5.0,$  and 0 mg:g. The respective times were 10, 30, 55,85, 115, 320, and 1230 minutes. The dispersion curves are fit with two relaxations alpha1 and alpha2 with respective magnitudes  $\Delta\epsilon_1$  and  $\Delta\epsilon_2$ . and relaxation times  $\tau_2$  and  $\tau_1$ .  $\Delta\epsilon_2$  decrease with decreasing water content and  $\Delta\epsilon_1$  remains constant. Plots of (c)  $\Delta\epsilon_2$  and  $\tau_2$  and (d)  $\tau_1$  versus  $f_w$  are also shown.
- Figure 6 An Arrhenius temperature plot of  $\tau_1$  used to fit the

hematite data and of  $\tau_1$  for magnetite with concentrations of <10% g/g in sand.

Figure 7 Dispersion curves of  $\epsilon'$  for various soils at 150 °C: 0.38 g cm<sup>-3</sup> Na-montmorillonite and  $f_w=0.019$ ; 0.51 g cm<sup>-3</sup> H-montmorillonite and  $f_w = 0.027$ ; 1.74 g cm<sup>-3</sup> test site soil and 0.019 g:g of H<sub>2</sub>O to clay (assuming 22 % clay); 0.73 g cm<sup>-3</sup> hematite; 1 % magnetite in sand of total density 1.35 g cm<sup>-3</sup>; and 1.35 g cm<sup>-3</sup> of sand.



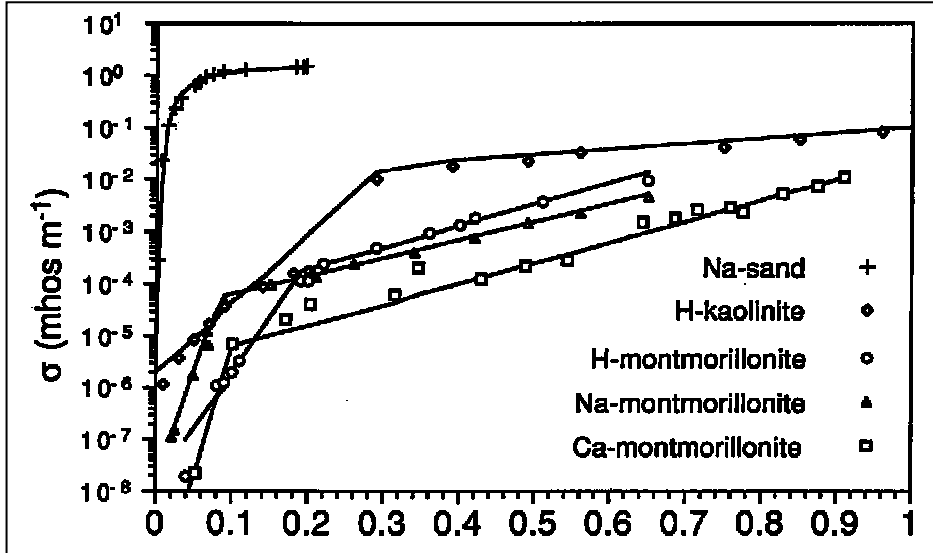
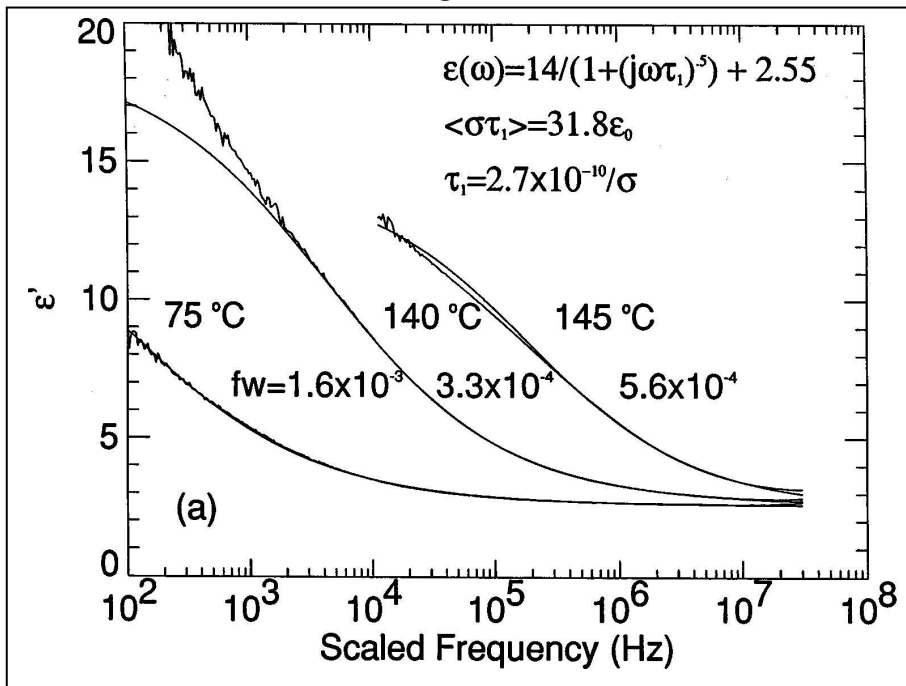


Figure 1



(a)

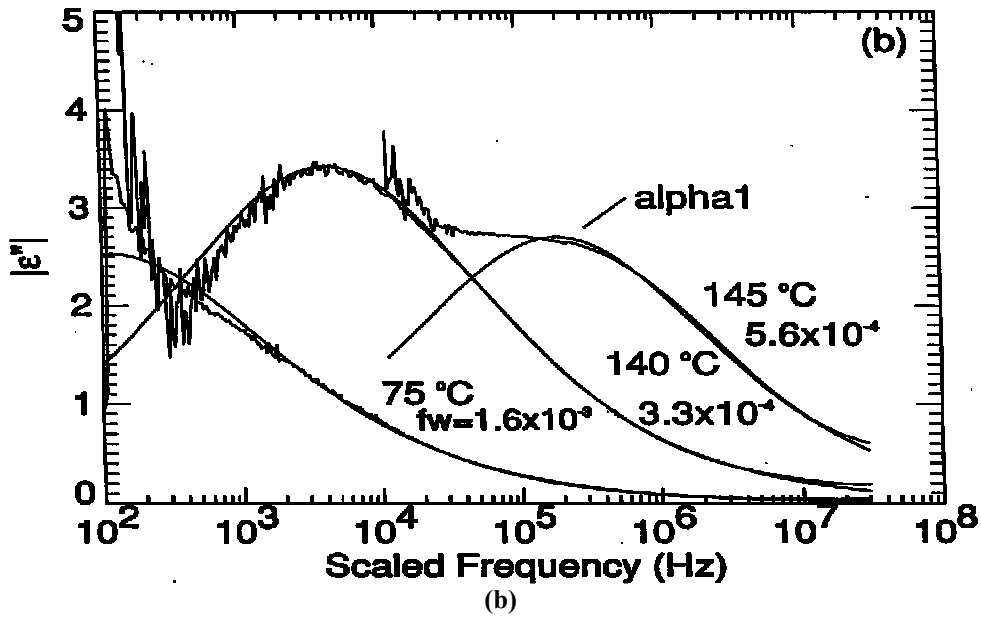


Figure 2

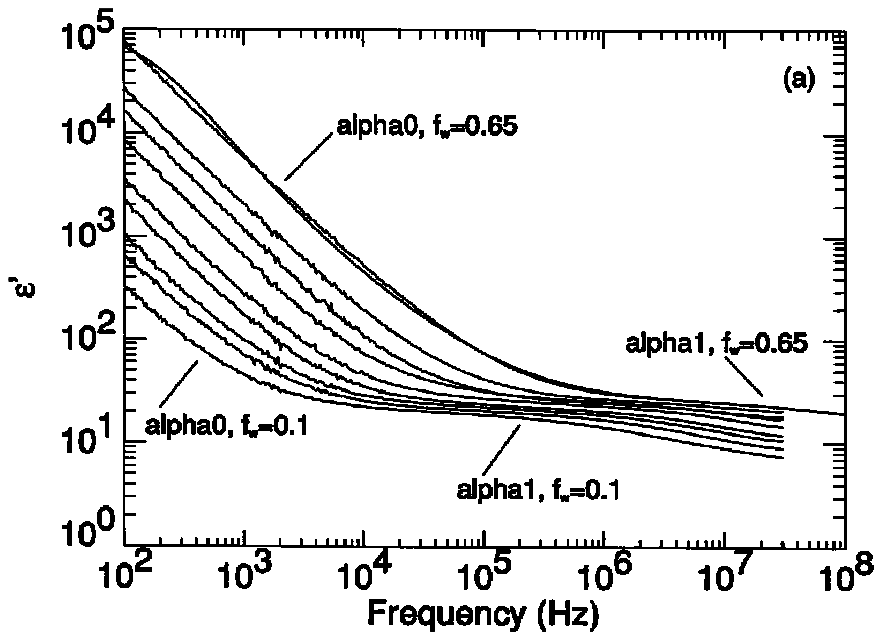
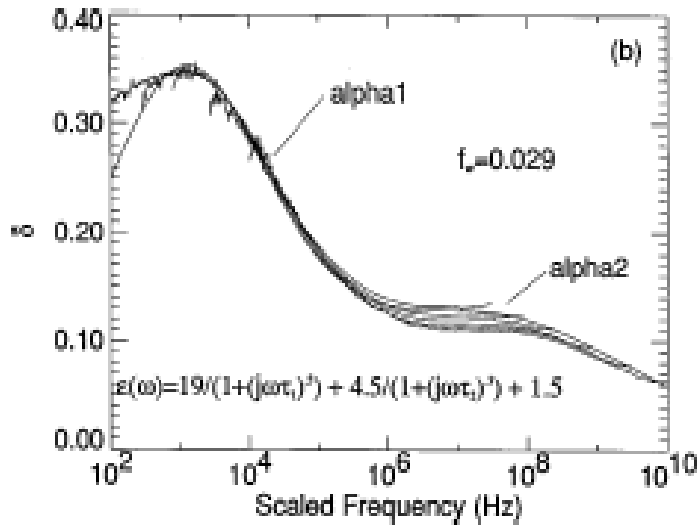
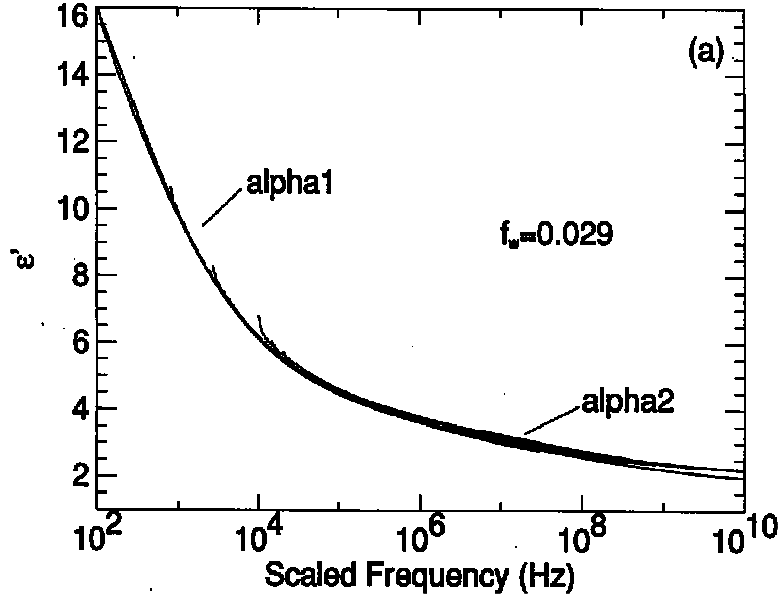
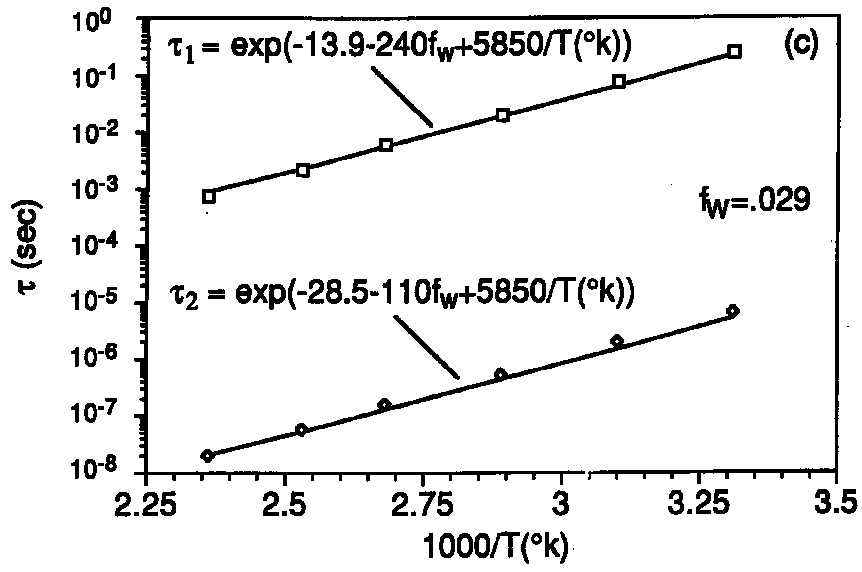


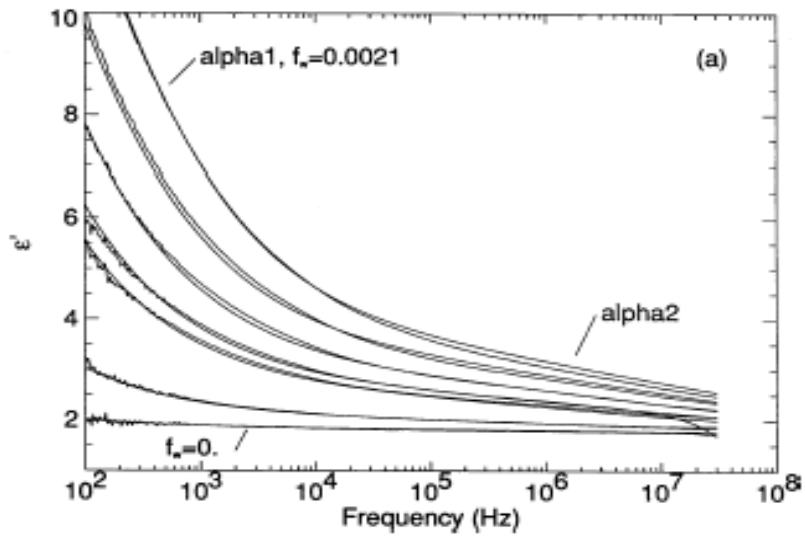
Figure 3



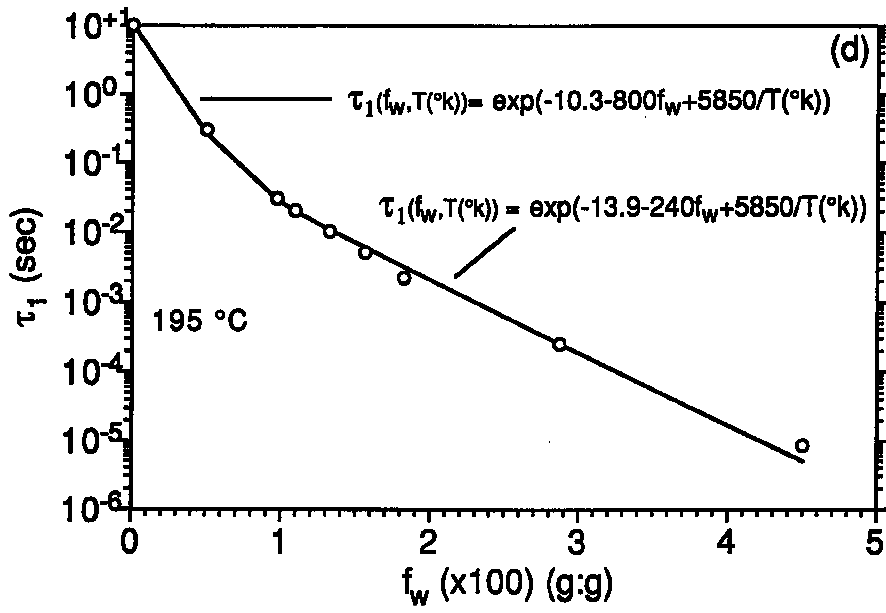
(b)



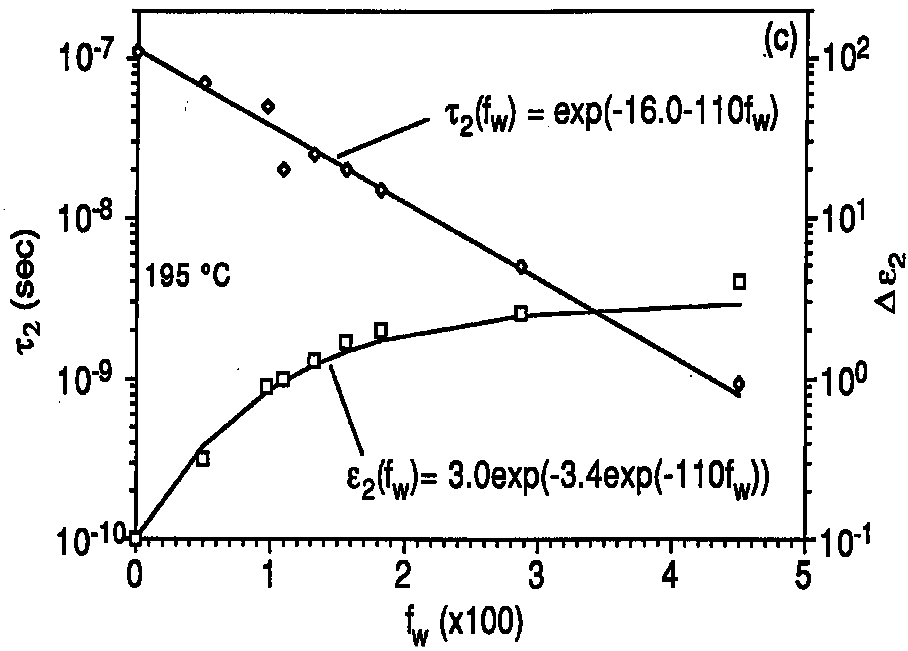
(c)  
Figure 4



(a)



(b)



(c)

Figure 5

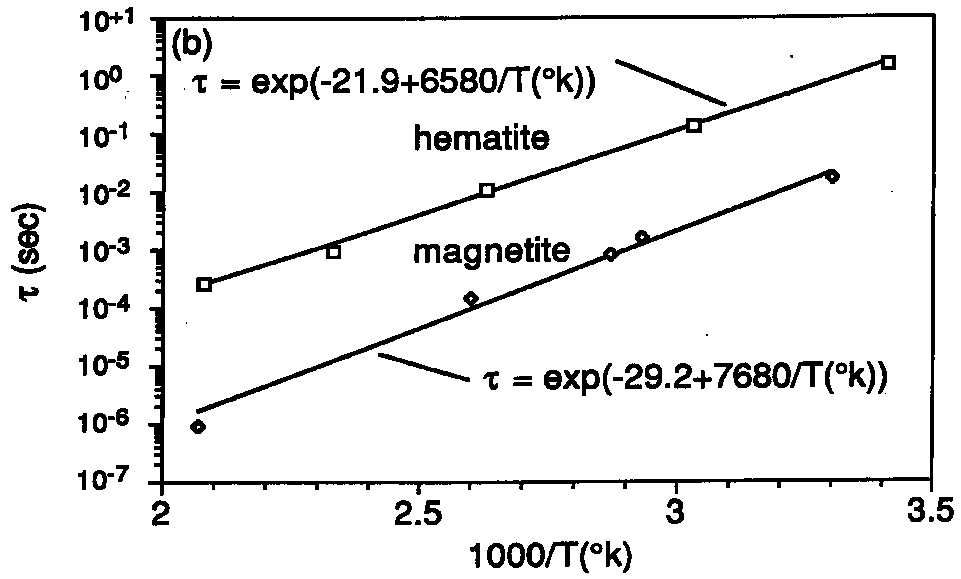


Figure 6

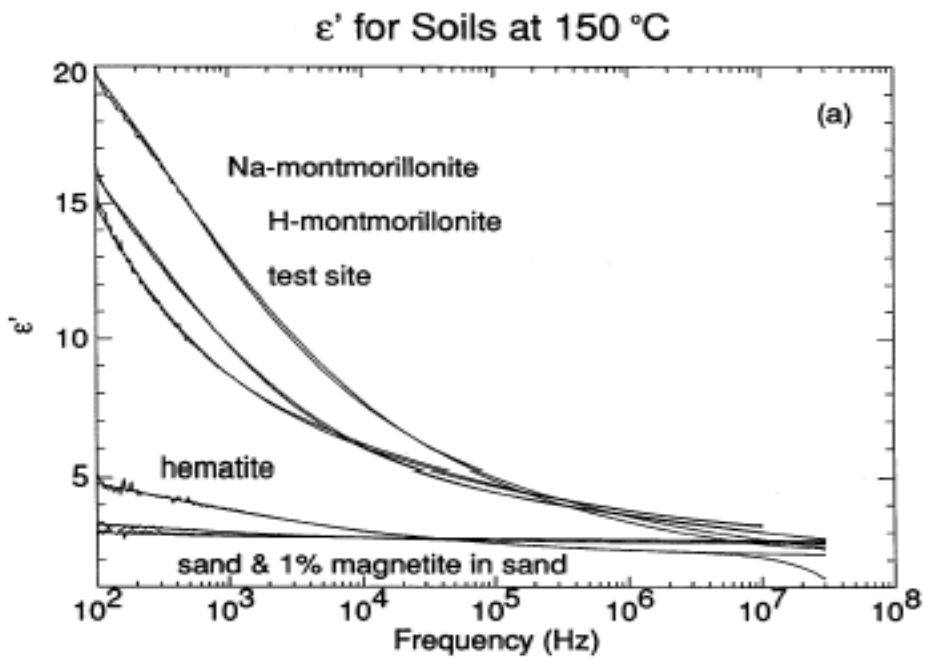


Figure 7